Endocrine Journal 2011, **58** (2), 117-121

ORIGINAL

GATA3 abnormalities in six patients with HDR syndrome

Maki Fukami[1], Koji Muroya[2], Tetsuo Miyake [1),3)], Manami Iso[1], Fumiko Kato[1], Hisashi Yokoi[4], Yoshimi Suzuki[5], Koji Tsubouchi[6], Yoshiko Nakagomi[7], Nobuyuki Kikuchi[8], Reiko Horikawa[9] and Tsutomu Ogata[1]

[1] *Department of Molecular Endocrinology, National Research Institute for Child Health and Development, Tokyo 157-8535, Japan*
[2] *Department of Endocrinology and Metabolism, Kanagawa Children's Medical Center, Yokohama 232-8555, Japan*
[3] *Department of Pediatrics, St. Marianna University Hospital, Kawasaki 216-8511, Japan*
[4] *Department of Internal Medicine, Japanese Red Cross Nagoya First Hospital, Nagoya 453-8511, Japan*
[5] *Department of Pediatrics, Atsumi Hospital, Tawara 441-3415, Japan*
[6] *Department of Pediatrics, Mino Municipal Hospital, Mino 501-3746, Japan*
[7] *Department of Pediatrics, Yamanashi University Hospital, Yamanashi 400-8510, Japan*
[8] *Department of Pediatrics, Yokohama City University Hospital, Yokohama 232-0024, Japan*
[9] *Division of Endocrinology and Metabolism, National Medical Center for Children and Mothers, Tokyo 157-8535, Japan*

Abstract. *GATA3* mutations cause HDR (*h*ypoparathyroidism, sensorineural *d*eafness, and *r*enal dysplasia) syndrome and, consistent with the presence of the second DiGeorge syndrome locus (*DGS2*) proximal to *GATA3*, distal 10p deletions often leads to HDR and DiGeorge syndromes. Here, we report on six Japanese patients with *GATA3* abnormalities. Cases 1–5 had a normal karyotype, and case 6 had a 46,XX,del(10)(p15) karyotype. Cases 1–6 had two or three of the HDR triad features. Case 6 had no DiGeorge syndrome phenotype except for hypoparathyroidism common to HDR and DiGeorge syndromes. Mutation analysis showed heterozygous *GATA3* mutations in cases 1–5, i.e., c.404–405insC (p.P135fsX303) in case 1, c.700T>C & c.708–709insC (p.F234L & p.S237fsX303) on the same allele in case 2, c.737-738insG (p.G246fsX303) in case 3, c.824G>T (p.W275L) in case 4, and IVS5+1G>C (splice error) in case 5. Deletion analysis of chromosome 10p revealed loss of *GATA3* and preservation of *D10S547* in case 6. The results are consistent with the previous finding that *GATA3* mutations are usually identified in patients with two or three of the HDR triad features, and provide supportive data for the mapping of *DGS2* in the region proximal to *D10S547*.

Key words: HDR syndrome, *GATA3*, DiGeorge syndrome, *DGS2*, Phenotypic spectrum

HDR (*h*ypoparathyroidism, sensorineural *d*eafness, and *r*enal dysplasia) syndrome is an autosomal dominant disorder first reported by Bilous *et al.* [1]. This condition is primarily caused by haploinsufficiency of *GATA3* on chromosome 10p15, although *GATA3* mutations have not been identified in a small portion of patients with clinical features compatible with HDR syndrome [2, 3]. *GATA3* consists of six exons, and encodes a transcription factor with two transactivating domains and two zinc finger domains on exons 2–6 [2]. *GATA3* is expressed in the developing parathyroid glands, inner ears, and kidneys, together with thymus and central nervous system (CNS) [4, 5].

Distal 10p deletions involving *GATA3* often lead to DiGeorge syndrome associated with hypoplastic thymus, T-cell immunodeficiency, hypoparathyroidism, congenital cardiac defects, and facial dysmorphism, in addition to HDR syndrome [6, 7]. Thus, deletion mappings have been performed, localizing the second DiGeorge syndrome locus (*DGS2*) to a ~1 cM region proximal to *D10S547* (the locus order: 10pter–*GATA3*–*D10S547*–*DGS2*–10cen) [6, 7].

Here, we report clinical and molecular findings in five patients with intragenic *GATA3* mutations and one patient with distal 10p deletion involving *GATA3*, and discuss the clinical features in *GATA3* mutation posi-

Received Aug. 4, 2010; Accepted Dec. 16, 2010 as K10E-234
Released online in J-STAGE as advance publication Jan. 13, 2011

Correspondence to: Tsutomu Ogata, Department of Molecular Endocrinology, National Research Institute for Child Health and Development, 2-10-1 Okura Setagaya-ku, Tokyo 157-8535, Japan.
E-mail: tomogata@nch.go.jp

Table 1 Summary of six patients with *GATA3* mutation or deletion

	Case 1	Case 2	Case 3	Case 4	Case 5	Case 6
Present age	40 years	39 years	4 years	31 years	17 years	4 years
Sex	Female	Female	Male	Female	Male	Female
Karyotype	46,XX	46,XX	46,XY	46,XX	46,XY	46,XX,del(10)(p15)
Hypoparathyroidism	Yes	Yes	Yes	Yes	Yes	Yes
Symptom	Convulsion	Tetany	No[b]	Convulsion	Convulsion	Convulsion
Ca (mg/dL)	3.4	3.4	2.7	4.3	3.0	4.7
P (mg/dL)	8.0	7.9	8.1	7.9	8.7	8.6
Intact PTH (pg/mL)	Undetected	Undetected	14	Undetected	Undetected	15
Age at diagnosis	10 years	13 years	17 months	3 years	17 months	2 weeks
Sensorineural deafness	Yes	Yes	No	Yes	Yes	Yes
Hearing level (dB)[a]	50 (B)	>70 (B)	Normal	60 (B)	50 (B)	90 (B)
Age at diagnosis	13 years	6 years		11 years	12 months	6 months
Renal lesion	Yes	Yes	Yes	Equivocal[c]	Yes	Yes
Malformation	RH (L)	PCD (B)	PD (R)	Absent	RH (L)	VUR (B)
Age at diagnosis	9 years	27 years	17 months		17 months	2 months

Abbreviations: PTH, parathyroid hormone; dB, decibel; B, bilateral; L, left; R, right; RH, renal hypoplasia; PCD, pelvicalyceal deformity; PD, pelvic duplication; and VUR, vesicoureteral reflux.
[a] Degree of hearing loss: normal, <25 dB; mild 26–40 dB; moderate 41–55 dB; moderately severe, 56–70 dB; and profound, >90 dB.
[b] Hypocalcemia was revealed by routine biochemical studies, when this boy was admitted because of bronchopneumonia.
[c] Renal malformation was absent, but renal dysfunction with increased serum creatinine was noticed during pregnancy.
Normal reference data: Ca: 8.84–10.44 mg/dL; P: 4.5–6.5 mg/dL; and intact PTH: 10–65 pg/mL.

tive patients and the chromosomal location of *DGS2*.

Patients and Methods

Patients

We studied six hitherto unreported Japanese patients (cases 1–6) with two or three HDR triad features. Cases 1–5 had a normal karyotype, and case 6 had a 46,XX,del(10)(p15) karyotype. Cases 1–4 and 6 were apparently sporadic cases, whereas case 5 was a possible familial case: the father received renal dialysis due to chronic renal failure from his twenties, and the paternal grandmother had unilateral renal hypoplasia, although they lacked clinical features suggestive of hypoparathyroidism and hearing difficulty.

Clinical phenotypes of the HDR triad features are summarized in Table 1. Hypoparathyroidism was noticed by convulsion in cases 1 and 4–6 and by tetany in case 2; in case 3, it was incidentally found by biochemical examinations at the time of admission due to bronchopneumonia. After confirming parathyroid hormone deficiency, 1α(OH) vitamin D therapy was started, successfully normalizing serum calcium and phosphate values in cases 1–6. Sensorineural deafness was demonstrated in cases 1, 2, and 4–6 by auditory brainstem response or audiometry, and they required hearing aids in their daily life. Case 3 had no hearing difficulty with normal auditory brainstem response. Renal lesion was radiologically confirmed in cases 1–3, 5, and 6. Although case 4 had no discernible renal malformation, she manifested renal dysfunction during pregnancy. In addition, case 6 exhibited developmental delay but lacked hypoplastic thymus, T-cell immunodeficiency, congenital cardiac defects, and facial dysmorphism characteristic of DiGeorge syndrome.

Mutation analysis of GATA3

This study was approved by the Institutional Review Board Committee at National Center for Child Health and Development. After obtaining informed consent, leukocyte genomic DNA samples of cases 1–6 were amplified by PCR for the coding regions on exons 2–6 and their flanking splice sites, and the PCR products were subjected to direct sequencing from both directions on a CEQ 8000 autosequencer (Beckman Coulter, Fullerton, CA). The primer sequences and the PCR conditions were as described previously [2, 3]. To confirm a heterozygous mutation, the corresponding PCR products were subcloned with a TOPO TA Cloning Kit (Life Technologies, Carlsbad, CA), and normal and mutant alleles were sequenced separately.

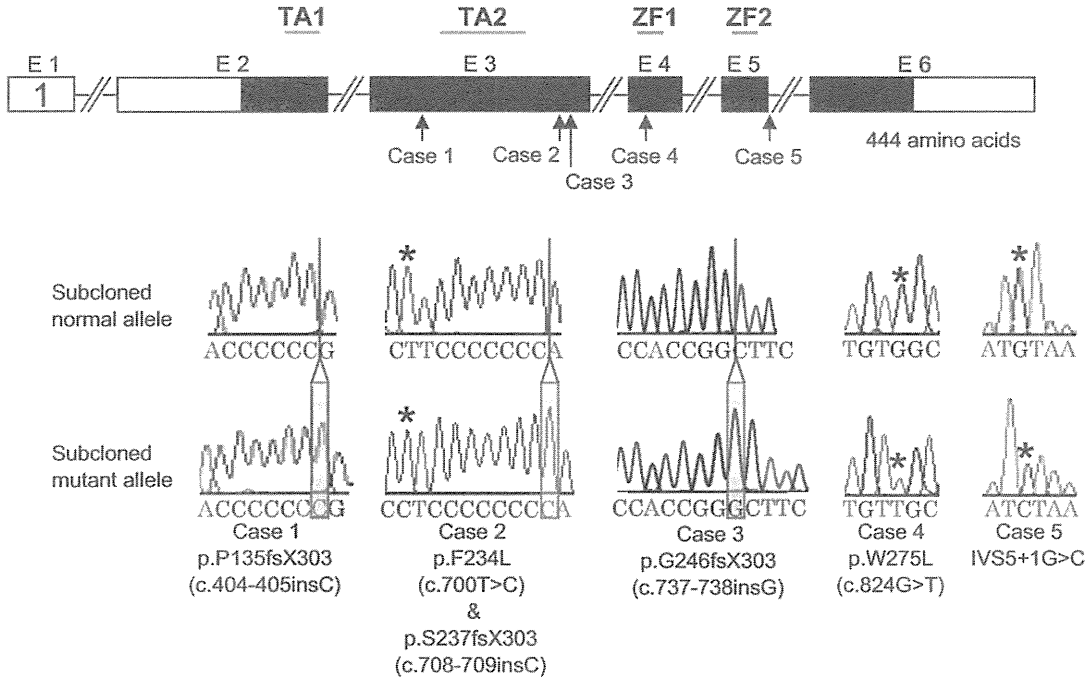

Fig. 1 Mutation analysis of *GATA3*.
Upper part: The structure of *GATA3* and the position of the mutations identified in cases 1–5. *GATA3* consists of exons 1–6 (E1–E6) and encodes two transactivating domains (TA1 and TA2) and two zinc finger domains (ZF1 and ZF2). The black and white boxes denote the coding regions and the untranslated regions, respectively.
Lower part: Electrochromatograms showing the subcloned normal and mutant sequences in cases 1–5.

Deletion analysis of 10p

To indicate an extent of the 10p deletion in case 6, oligoarray comparative genomic hybridization (CGH) was carried out with 1x244K Human Genome Array (catalog No. G4411B) (Agilent Technologies, Palo Alto, CA), according to the manufacturer's protocol. Furthermore, fluorescence *in situ* hybridization (FISH) was performed with an RP11-554F11 BAC probe containing the whole *GATA3* gene [3] and an RP11-17E09 BAC probe containing *D10S547* (BACPAC Resources Center, Oakland, CA), together with a CEP 10 probe for *D10Z1* (Abbott, Chicago, IL) utilized as an internal control. The two BAC probes were labeled with digoxigenin and detected by rhodamine anti-digoxigenin, and the control probe was detected according to the manufacturer's protocol.

Results

Mutation analysis of GATA3

Direct sequencing identified heterozygous *GATA3* mutations in cases 1–5, i.e., a frameshift mutation (c.404–405insC, p.P135fsX303) in case 1, a missense mutation (c.700T>C, p.F234L) and a frameshift mutation (c.708–709insC, p.S237fsX303) on the same allele in case 2, a frameshift mutation (c.737-738insG, p.G246fsX303) in case 3, a missense mutation (c.824G>T, p.W275L) in case 4, and a splice donor site mutation (IVS5+1G>C) in case 5 (Fig. 1). Unfortunately, the renal phenotype positive father and paternal grandmother of case 5 were not examined. These mutations were absent from 200 control subjects. No intragenic mutation was identified in case 6 with distal 10p deletion.

Deletion analysis of 10p

CGH revealed a ~10 Mb terminal deletion from chromosome 10p of case 6 (Fig. 2). FISH analysis showed that the 10p deletion chromosome was missing *GATA3* and retained *D10S547*.

Discussion

Cases 1–6 had two or three of the HDR triad features and heterozygous *GATA3* abnormalities. This is consistent with the previous notion that *GATA3* mutations

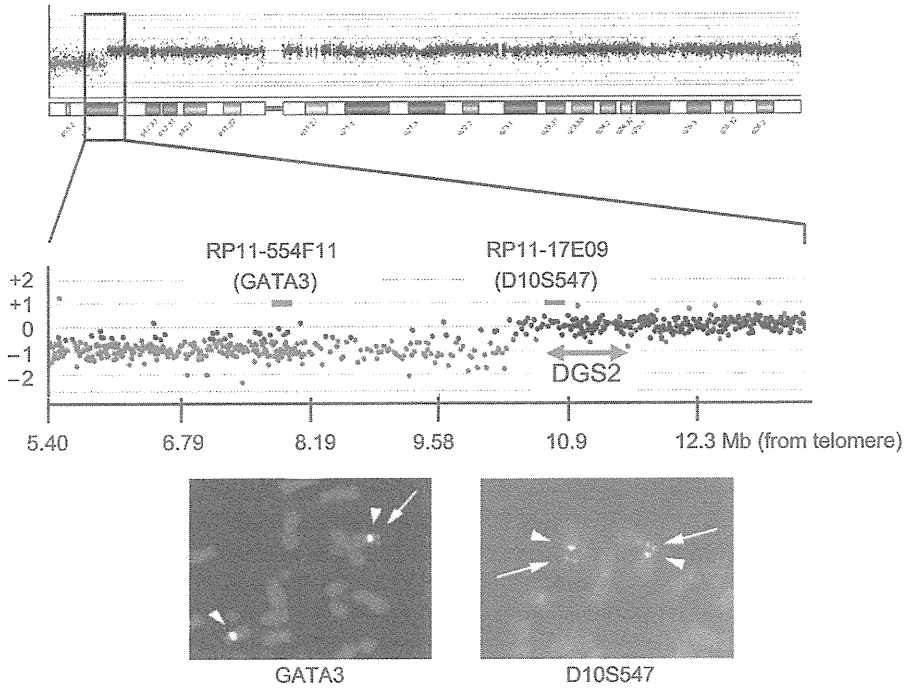

Fig. 2 Deletion analysis of 10p. The green and black signals in CGH indicate the deleted and preserved regions on the 10p deleted chromosome, respectively. The critical region for *DGS2* is indicated. The RP11-554F11 probe containing *GATA3* detects only a single signal (an arrow), whereas the RP11-17E09 probe containing *D10S547* identifies two signals (arrows). The arrowheads indicate *D10Z1* detected by a control CEP 10 probe.

are usually identified in patients with two or three of the HDR triad features [8, 9]. However, this would more or less be due to an ascertainment bias that *GATA3* are usually examined in patients diagnosed as having HDR syndrome. Indeed, familial studies of probands with typical HDR syndrome have identified *GATA3* mutations in subjects with apparently deafness only phenotype [3, 10], although there has been no report documenting apparently normal phenotype in individuals with *GATA3* mutations. It is possible, therefore, that *GATA3* mutations are associated with a relatively wide penetrance and expressivity of the HDR triad features. In this context, it is notable that the father and the paternal grandmother of case 5 had renal abnormalities as the sole discernible clinical phenotype. This suggests that *GATA3* mutations may cause renal abnormalities alone in exceptional patients, although mutations analysis could not be performed for the father and the grandmother.

Case 6 lacked T-cell immunodeficiency, congenital cardiac defects, and abnormal facial appearance characteristic of DiGeorge syndrome. While case 6 had hypoparathyroidism, this is explained by loss of *GATA3*. In addition, developmental delay is ascribed to chromosome aberration. Thus, genotype-phenotype correlation in case 6 is consistent with the previous mapping of *DGS2* to a region proximal to *D10S547* [6, 7].

Acknowledgements

This work was supported by Grants for Child Health and Development and for Research on Children and Families from the Ministry of Health, Labor, and Welfare.

References

1. Bilous RW, Murty G, Parkinson DB, Thakker RV, Coulthand MG, Burn J, Mathias D, Kendall-Tailor P (1992) Autosomal dominant familial hypoparathyroidism, sensorineural deafness, and renal dysplasia. *N Engl J Med* 327: 1069–1074.
2. Van Esch H, Groenen P, Nesbit MA, Schuffenhauer S,

Lichtner P, Vanderlinden G, Harding B, Beetz R, Bilous RW, Holdaway I, Shaw NJ, Fryns JP, Van de Ven W, Thakker RV, Devriendt K (2000) GATA3 haplo-insufficiency causes human HDR syndrome. *Nature* 406: 419–422.

3. Muroya K, Hasegawa T, Ito Y, Nagai T, Isotani H, Iwata Y, Yamamoto K, Fujimoto S, Seishu S, Fukushima Y, Hasegawa Y, Ogata T (2001) GATA3 abnormalities and the phenotypic spectrum of HDR syndrome. *J Med Genet* 38: 374–380.
4. Labastie MC, Catala M, Gregoire JM, Peault B (1995) The GATA3 gene is expressed during human kidney embryogenesis. *Kidney Int* 47: 1597–1603.
5. Debacker C, Catala M, Labastie MC (1999) Embryonic expression of the human GATA3 gene. *Mech Dev* 85: 183–187.
6. Schuffenhauer S, Lichtner P, Peykar-Derakhshandeh P, Murken J, Haas OA, Back E, Wolff G, Zabel B, Barisic I, Rauch A, Borochowitz Z, Dallapiccola B, Ross M, Meitinger T (1998) Deletion mapping on chromosome 10p and definition of a critical region for the second DiGeorge syndrome locus (DGS2). *Eur J Hum Genet* 6: 213–225.
7. Lichtner P, König R, Hasegawa T, Van Esch H, Meitinger T, Schuffenhauer S (2000) An HDR (hypoparathyroidism, deafness, renal dysplasia) syndrome locus maps distal to the DiGeorge syndrome region on 10p13/14. *J Med Genet* 37: 33–37.
8. Nesbit MA, Bowl MR, Harding B, Ali A, Ayala A, Crowe C, Dobbie A, Hampson G, Holdaway I, Levine MA, McWilliams R, Rigden S, Sampson J, Williams AJ, Thakker RV (2004) Characterization of GATA3 mutations in the hypoparathyroidism, deafness, and renal dysplasia (HDR) syndrome. *J Biol Chem* 279: 22624–22634.
9. Ali A, Christie PT, Grigorieva IV, Harding B, Van Esch H, Ahmed SF, Bitner-Glindzicz M, Blind E, Bloch C, Christin P, Clayton P, Gecz J, Gilbert-Dussardier B, Guillen-Navarro E, Hackett A, Halac I, Hendy GN, Lalloo F, Mache CJ, Mughal Z, Ong AC, Rinat C, Shaw N, Smithson SF, Tolmie J, Weill J, Nesbit MA, Thakker RV (2007) Functional characterization of GATA3 mutations causing the hypoparathyroidism-deafness-renal (HDR) dysplasia syndrome: insight into mechanisms of DNA binding by the GATA3 transcription factor. *Hum Mol Genet* 16: 265–275.
10. Chiu WY, Chen HW, Chao HW, Yann LT, Tsai KS (2006) Identification of three novel mutations in the GATA3 gene responsible for familial hypoparathyroidism and deafness in the Chinese population. *J Clin Endocrinol Metab* 91: 4587–4592.

Pediatr Radiol
DOI 10.1007/s00247-011-2132-1

ORIGINAL ARTICLE

Radiological evaluation of dysmorphic thorax of paternal uniparental disomy 14

Osamu Miyazaki · Gen Nishimura · Masayo Kagami · Tsutomu Ogata

Received: 21 November 2010 / Revised: 31 January 2011 / Accepted: 1 February 2011

Abstract
Background The "coat-hanger" sign of the ribs with a bell-shaped thorax has been known as a radiological hallmark of the paternal uniparental disomy 14 (upd(14)pat).
Objective To quantitatively determine the differences in thoracic deformity between upd(14)pat and other bone diseases with thoracic hypoplasia and to establish the age-dependent evolution.
Materials and methods The subjects comprised 11 children with upd(14)pat. The angle between the 6th posterior rib and the horizontal axis was measured (coat hanger angle; CHA). The ratio of the mid- to widest thorax diameter (M/W ratio) was calculated for the bell-shaped thorax.
Results CHA ranged from +28.5 to 45° (mean; 35.1°±5.2) in upd(14)pat, and from −19.8 to 21° (−3.3±13°) in bone dysplasias ($p<0.01$). The M/W ratio ranged from 58% to 93% (75.4±10) in upd(14)pat, and from 80% to 92% (86.8±3.3) in bone dysplasias ($p<0.05$). Serial radiographs revealed that CHA remained constant during early childhood, while the M/W ratio gradually increased with age.
Conclusion The "coat-hanger" sign of upd(14)pat provides a distinctive radiological gestalt that makes it possible to differentiate the disorder from other skeletal dysplasias. By contrast, the bell-shaped thorax is significant only in the neonatal period.

Keywords UPD14 · Plain radiograph · Coat-hanger sign · Bell-shaped thorax

O. Miyazaki (✉)
Department of Radiology,
National Center for Child Health and Development,
2-10-1 Okura,
Seatagaya-ku, Tokyo 157-8535, Japan
e-mail: osamu-m@rc4.so-net.ne.jp

G. Nishimura
Department of Radiology,
Tokyo Metropolitan Children's Medical Center,
2-8-29 Musashidai,
Fuchu-shi, Tokyo 183-8561, Japan

M. Kagami · T. Ogata
Division of Clinical Genetics and Molecular Medicine,
National Center for Child Health and Development,
2-10-1 Okura,
Seatagaya-ku, Tokyo 157-8535, Japan

Published online: 24 May 2011

Introduction

Uniparental disomy (UPD) refers to the inheritance of a pair of chromosomes from only one parent. UPD is a relatively common phenomenon. The inheritance of both, or parts of both, maternal chromosomes (heterodisomic maternal UPD) has been found to become more prevalent as parental age becomes more advanced [1]. It is well established that UPD for chromosomes 6, 7, 11, 14 and 15 is associated with recognized syndromes, including Prader-Willi syndrome (maternal UPD 15), Angelman syndrome (paternal UPD 15), and Beckwith-Wiedemann syndrome (paternal UPD 11) [2].

The paternal UPD 14 phenotype (upd(14)pat) is a recently recognized genetic condition that is caused by an aberration of the imprinting center in chromosome 14. The clinical hallmarks of upd(14)pat are thoracic hypoplasia and abdominal wall defect. Mild facial dysmorphism and developmental delay are also noted. In addition, upd(14)pat presents with a distinctive radiological finding: the "coat-hanger" appearance of the ribs and a bell-shaped thorax [3]. In the past, upd(14)pat was often misdiagnosed as bone dysplasias with thoracic hypoplasia, as in Jeune syndrome [4], because attention was not paid to the morphological differences of the thorax between upd(14)pat and other genetic bone diseases. Previous reports on

upd(14)pat have been based on a single case or a limited number of cases. To date, there has been no radiological report involving a large series of upd(14)pat cases. Although a previous report suggested that the dysmorphic thorax in upd(14)pat ameliorated in the mid-childhood period [5], it remains to be determined how the thoracic deformity in upd (14)pat evolves with age. The purpose of this study was to quantitatively determine the differences in the thoracic deformity between upd(14)pat and other genetic bone diseases, and to establish the age-dependent radiological evolution of the thoracic hypoplasia in upd(14)pat.

Materials and methods

The subjects comprised 11 children (6 girls and 5 boys) with upd(14)pat phenotypes proven on molecular grounds [5, 6]. Three of the 11 children had been managed in our hospital, and 8 were referred to our institution for molecular diagnosis. The molecular diagnoses included seven cases of paternal uniparental disomy, two of microdeletion and two of epimutation. The initial radiographs available for the analysis were obtained in the neonatal period (n=8), and at 7, 24 and 32 months of age (n=1). Sequential radiological evaluation was feasible in 4 of 11 children up to 5 years of age. The study was approved by the institutional review board at the National Center for Child Health and Development.

To assess for the "coat-hanger" sign, the angle between the 6th posterior rib and the horizontal axis was measured (coat hanger angle, CHA; an upward angle was defined as +, and a downward angle as −). The ratio of the mid- to widest thorax diameter (M/W ratio) was calculated for the bell-shaped thorax (Figs. 1, 2). For comparison, both indexes were evaluated in nine cases with bone dysplasia with thoracic hypoplasia, including thanatophoric dysplasia (n=6), Ellis-van Creveld syndrome (n=2) and asphyxiating thoracic dysplasia (n=1). These cases were selected from our radiology database. The children's ages ranged from 21 weeks of gestation to 6 years of age (mean: 11 months of age). Both indexes were also evaluated in five children with respiratory distress syndrome (RDS) and without skeletal abnormalities that could be assessed to determine the evolution of the normal thoracic morphology. In the RDS group, serial follow-up radiographs were available from the neonatal period up to 2 years to 6 years of age (mean 4.2). The measurement of CHA and M/W ratio was performed using an accessory digital tool from a PACS

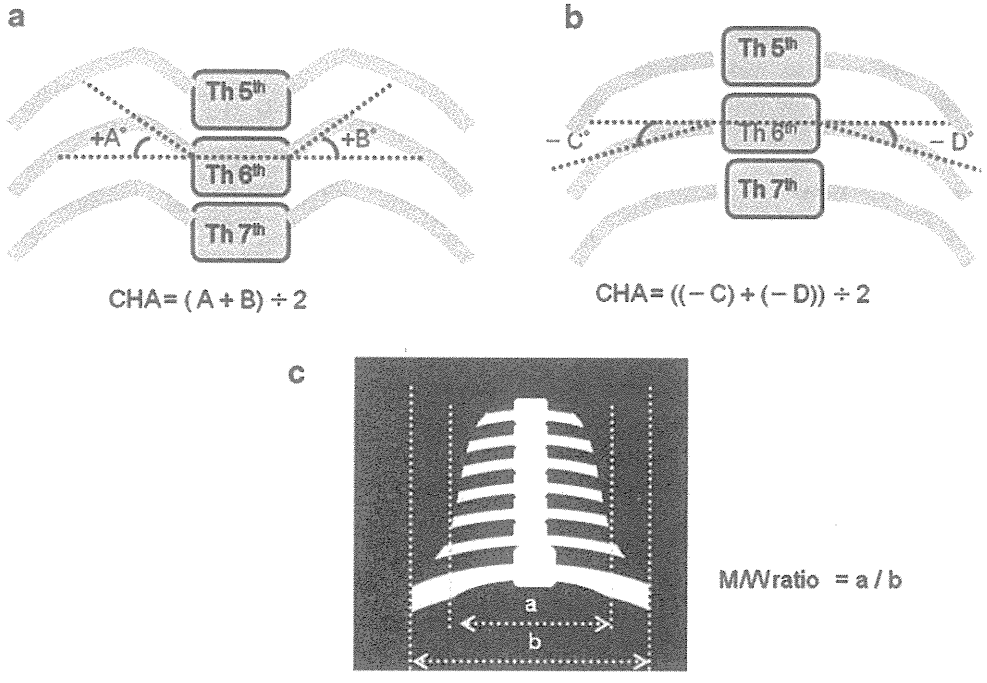

Fig. 1 **a, b** Diagram of coat-hanger angle (CHA) and mid/widest ratio. CHA refers to the average of the angles between the peak point of both 6th posterior ribs and the horizontal axis. If there is no peak point of the 6th posterior ribs, the center of the ribs is utilized instead. The horizontal axis is defined as a line passing through two points of both 6th cost-vertebral junctions. An upward angle is defined as +, and a downward angle as −. CHA is thought to be a quantitative index of the coat-hanger sign. **c** The ratio of mid- to widest thorax (M/W ratio) refers to the ratio of the narrowest diameter of the mid-thorax to the widest diameter of the basal thorax. In most cases with upd(14)pat, the thorax showed medial concavity with the top of approximately the 6th rib (the narrowest mid-thorax) and downward sloping toward the 9th to 11th ribs (the widest basal thorax). M/W ratio is thought to be a quantitative index of dysmorphic bell-shaped thorax

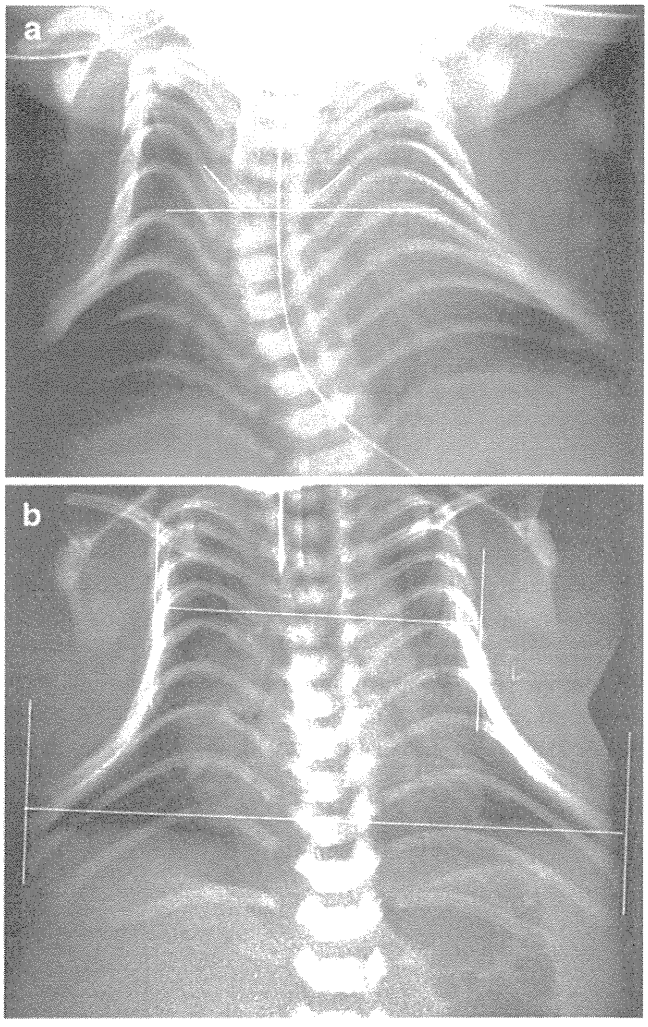

Fig. 2 Examples of CHA and M/W ratio. **a** The 6th posterior ribs show upward bowing that provides the coat-hanger sign. The CHA of this case (patient #7 in Table 1) was 45° (the measurement was 48° for the right and 42° for the left). **b** The M/W ratio was 58% in this case (patient #5 in Table 1). This is an example of severe bell-shaped thorax in upd(14)pat

system (Centricity ™ RA 1000 Ver.3.0, GE Healthcare, Milwaukee, WI) on the PACS monitor, or using area and protractor commercial software (Lenara Ver2.21, Vector, Tokyo) on a personal computer monitor. An unpaired two-tailed t-test was used for statistical evaluation.

Results

Clinical and measurement data are summarized in Table 1 and Fig. 3. All 11 children with upd(14)pat showed a severe upward sweep of the posterior rib or increased CHA, ranging from +28.5 to 45° (mean ± SD; 35.1°±5.2) (Figs. 2, 3). Children with bone dysplasias presented with variable manifestations of the posterior rib, and CHA ranged from −19.8 to 21° (mean ± SD; −3.3±13°) (Figs. 3, 4). The difference in CHA was statistically significant between the upd(14)pat and bone dysplasia groups ($P<0.01$). According to this result, approximately +25° was the estimated cut-off line of CHA to differentiate upd(14)pat from skeletal dysplasias (Fig. 3). The M/W ratio ranged from 58% to 93% (mean±SD; 75.4±10) in the upd(14)pat group, while it ranged between 80% and 92% (mean±SD; 86.8±3.3) in the skeletal dysplasia group (Fig. 3). The difference an unpaired two-tailed t-test in the M/W ratio was, though statistically significant, less conspicuous than that in CHA ($P<0.05$). There was considerable overlap in the range of the M/W ratio between the upd(14)pat and skeletal dysplasia groups.

The age-dependent evolution of CHA and M/W ratio in the upd(14)pat and RDS groups is shown in Fig. 5. In the four children with upd(14)pat, CHA remained unaltered regardless of age, ranging from 25° to 45°. In the RDS group ($n=5$), CHA was constant regardless of age, ranging from −6.4 to 10° (mean −0.6) at birth and from −8 to 7.3° thereafter (Fig. 5). The M/W ratio of the upd(14)pat group was smaller than that of the RDS group in the neonatal period. However, it increased gradually with age and finally caught up with that observed in the RDS group (Figs. 6, 7).

Discussion

The clinical manifestations of upd(14)pat have been well established to date. The hallmarks of this condition include a small thorax, laryngomalacia, hypoplastic abdominal wall, short limbs with joint contractures, craniofacial dysmorphism, and mental retardation [2]. In addition, several reports on the prenatal diagnosis of upd(14)pat suggested the common occurrence of polyhydramnios and preterm delivery in upd(14)pat [2, 7]. A few reports on upd (14)pat have detailed the radiological manifestations, such as disproportionately short limbs, spurring of lower femoral and upper tibial metaphyses, absent glenoid fossa, shortened iliac wing with flaring, thin and elongated clavicle, hypoplastic scapular neck, kyphoscoliosis, hypoplasia of the maxilla and mandible, a broad nasal bridge, wide sutures and multiple wormian skull bones, contractures of the wrists with ulnar deviation, and stippled calcification [3, 8–10]. However, these findings are so mild that alone they do not determine the diagnosis. Instead, the distinctive thoracic deformity in upd(14)pat, termed the coat-hanger sign as introduced by Offiah et al. [3], enables a definitive diagnosis to be made. Sutton et al. [8] described the thoracic deformity of upd(14)pat as "anterior ribs bowed caudally (downward), and posterior portions of the ribs bowed cranially (upward)," and these configurations are combined in the characteristic coat-hanger sign of the ribs

Table 1 Summary of clinical details, measurement of rib angle, coat-hanger angle (CHA), and ratio of mid- to widest thorax (M/W ratio). *GW* gestational week, *TD* thanatophoric dysplasia, *ATD* asphyxiating thoracic dysplasia, *EvC* Ellis-van Creveld syndrome, *RDS* respiratory distress syndrome

Case	Gender	Age (months)[a]	Molecular or clinical diagnosis	Right rib angle (°)	Left rib angle (°)	CHA (°)	M/W ratio (%)
upd(14)pat patients							
1	f	0	upd	36	31	33.5	80
2	m	0	upd	43	41	42	66
3	m	0	upd	27	46	36.5	80
4	m	7	upd	32	38	35	80
5	m	0	deletion	27	30	28.5	58
6	f	0	Epimutation	35	23	29	77
7	f	0	Epimutation	48	42	45	65
8	f (45,XX)	0	upd	30	34	32	69
9	f	0	upd	46	32	39	74
10	m	24	upd	28	38	33	87
11	f	32	decision	32	33	32.5	93
mean		5.7		35	35.82	35.1	75.4
TD group patients							
1	m	21GW	TD	−9.9	−13.7	−11.8	80
2	f	6	TD	−3.7	12	1	85.6
3	m	21GW	TD	−11.7	−13.9	−12.8	86
4	Unknown	20GW	TD	−19.6	−20	−19.8	86
5	m	0	TD	7	−12	−2.5	87
6	m	21GW	TD	−15	−21	−18	87
7	m	84	ATD	4	2	3	88
8	f	11	EvC	9.6	10.3	9.95	90
9	m	24	EvC	14	28	21	92
mean		11		−2.8	−3.1	−3.3	86.8
RDS patients							
1	m	0	RDS	1.8	4	2.9	90
2	m	0	RDS	1.2	−14	−6.4	81.7
3	m	0	RDS	−6.9	−4.1	−5.2	84
4	m	0	RDS	−6	−2	−4	91
5	f	0	RDS	11.3	8.7	10	85
mean		0		0.28	−1.48	−0.54	86.3

[a] Age at which time the initial radiograph was available

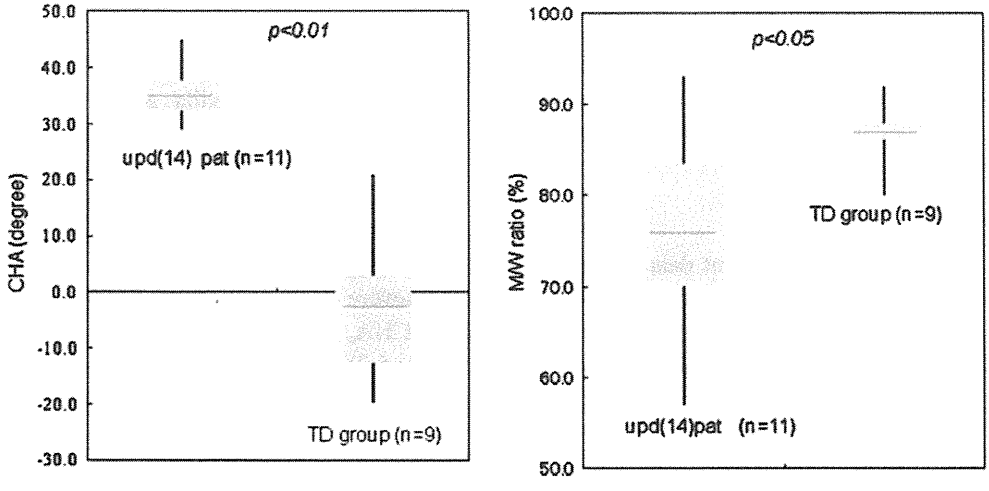

Fig. 3 Box plot of CHA and M/W ratio with the median, interquartile interval and range

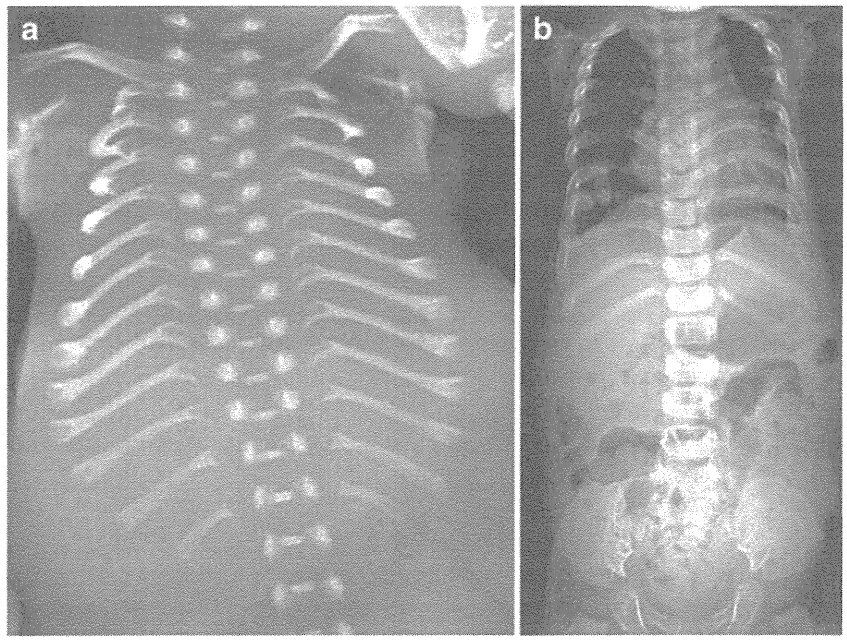

Fig. 4 Examples of the thoracic appearance and measurement of bone dysplasias with thoracic hypoplasia. **a** Thanatophoric dysplasia (TD) type 1 (stillbirth at 21 weeks of gestation). Note a narrow thorax with cupped anterior ends as well as short long bones with metaphyseal cupping. The posterior ribs show downward sloping. The CHA was −18°, and the M/W ratio was 87%. Despite the presence of severe thoracic hypoplasia in TD, its morphology is different from that seen in upd(14)pat (Fig. 2). **b** Ellis-van Creveld (EvC) syndrome (2 years of age). The thorax appears narrow, and a trident appearance of the acetabula is seen. Posterior ribs show upward sloping. The CHA was 21°, and the M/W ratio was 92%. The morphological pattern of the thorax differs from that of upd(14)pat

on the chest radiograph. Sutton et al. concluded that the skeletal phenotype in upd(14)pat involves primarily the axial skeleton, with little to no effect on the long bones. Very small changes of the long bones in upd(14)pat correspond with those of the mouse model (UPD of the distal segment of mouse chromosome 12) [11]. Consequently, it is assumed that imprinted genes on human chromosome 14 and mouse chromosome 12 play a role in axial skeletal formation and ossification [8, 11].

In the subsequent articles on upd(14)pat, all 11 affected children presented unexceptionally with the coat-hanger sign [5, 6, 12]. It was thought that the upward posterior rib bowing and downward anterior rib bowing (the coat-hanger appearance) in upd(14)pat contrast with the horizontally oriented ribs generally seen in disorders with thoracic hypoplasia. Based on the radiological sign, along with other radiological findings, it is not difficult to differentiate upd(14)pat from other genetic disorders involv-

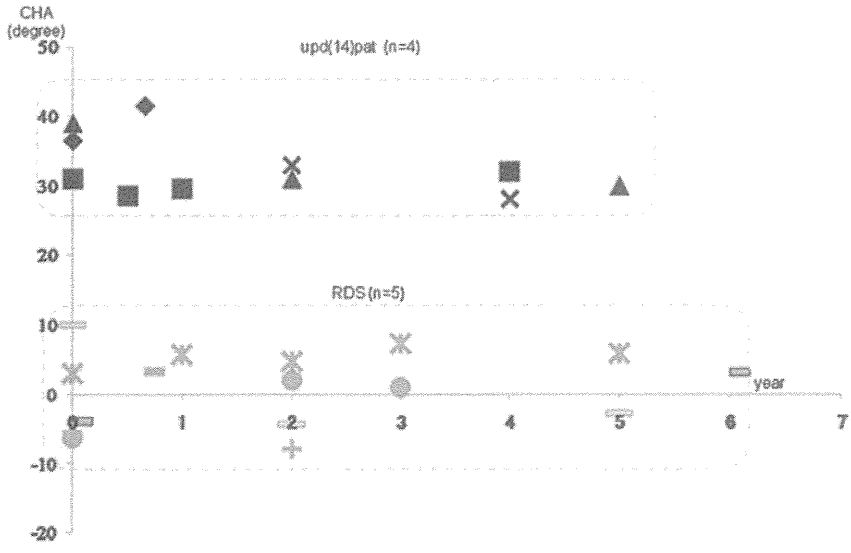

Fig. 5 Comparative observation of age-dependent transition of CHA between the upd(14)pat and respiratory distress syndrome (RDS) groups. Individual shapes represent individual patients

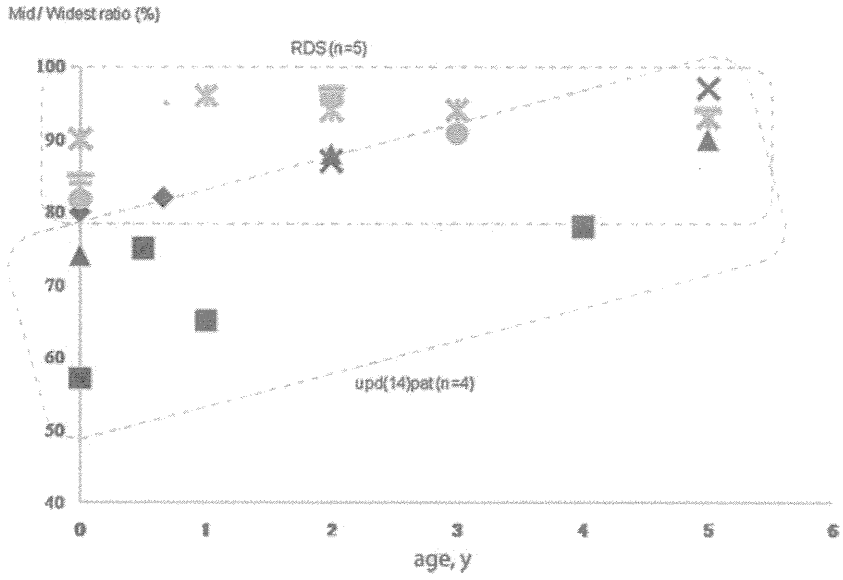

Fig. 6 Comparative observation of age-dependent transition of M/W ratio between the upd(14) pat and RDS groups. Individual shapes represent individual patients

ing thoracic hypoplasia, such as thanatophoric dysplasia, asphyxiating thoracic dysplasia and metatropic dysplasia [13]. However, there are several disorders wherein thoracic hypoplasia is the sole radiological hallmark, including Barnes syndrome, Shwachman-Diamond syndrome and the mildest cases of asphyxiating thoracic hypoplasia. Thus, we thought that quantitative analyses of the coat-hanger sign could elucidate how different the thoracic hypoplasia

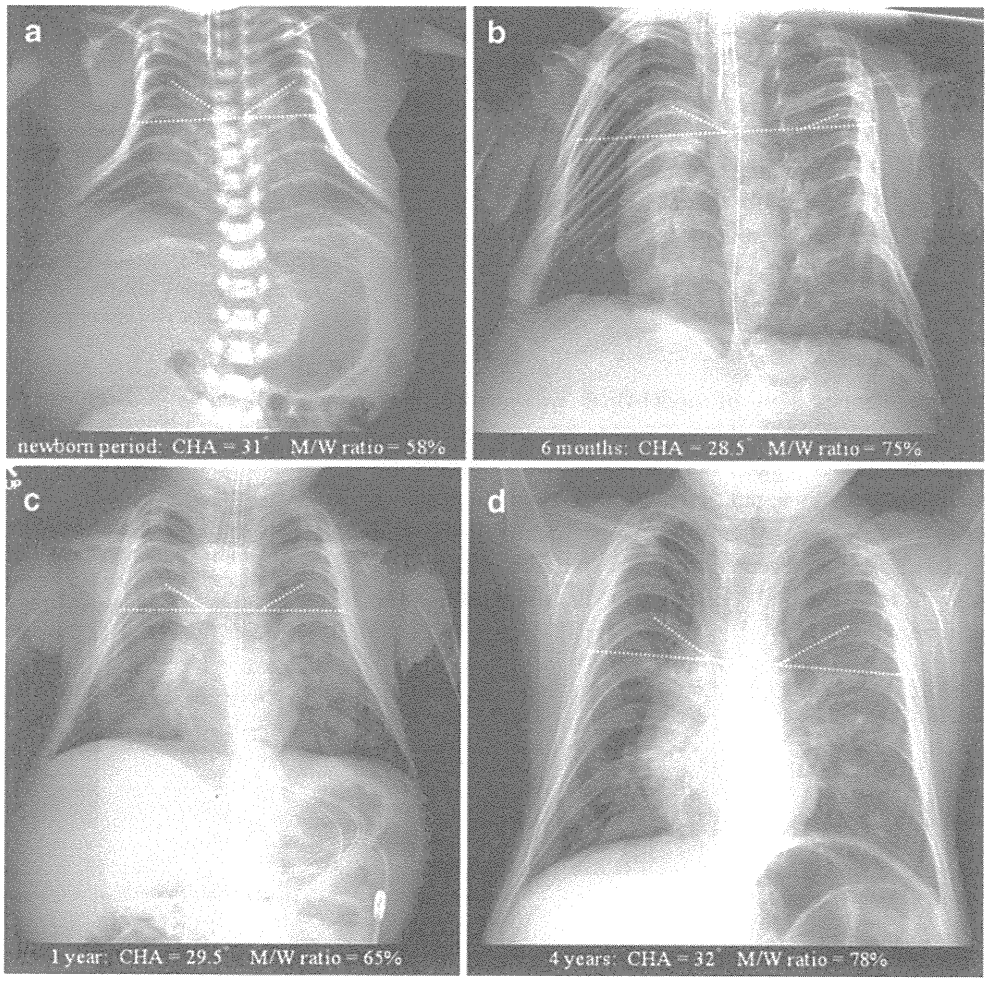

Fig. 7 Serial images of the thorax deformity in upd(14)pat. In this case, four images taken at different ages were available: (**a**) neonatal period, (**b**) 6 months, (**c**) 1 year and (**d**) 4 years. The CHA was almost consistent regardless of age, while the M/W ratio increased with advancing age. The coat-hanger sign and bell-shaped thorax are readily identifiable in the neonatal period. The diagnosis is not straightforward in childhood, yet close observation combined with CHA measurement points to the coat-hanger sign

in upd(14)pat is from the thoracic hypoplasia in other genetic disorders, and presumed that the measurement of CHA (mean 35.1°) and M/W ratio (mean 75.4%) might be helpful when the diagnosis of upd(14)pat is in question. As comparison groups, we included not only cases of severe bone dysplasias but also RDS. Neonates with RDS may present with a small chest [14], and it is not uncommon for them to undergo repeated examinations of chest radiographs because of the association with chronic lung disease.

Kagami et al. [5] reported the age-dependent evolution of the thoracic deformity of upd(14)pat in two children, which was said to ameliorate in mid-childhood. Their observation corresponded with the improvement of the M/W ratio with age described here. By contrast, however, CHA persisted consistently until mid-childhood. This finding indicates that the coat-hanger sign is still discernable during mid-childhood. Radiological findings are presumed to be the only clue to the presence of upd(14)pat after mid-childhood. Serial radiographs (newborn, 2 years and 9 years), as illustrated by Cotter et al. [15] also warrant our observation.

A drawback of this study is that it includes a limited number of cases and available radiographs with uneven quality, such as chest radiographs with some obliquity and radiographs taken in the supine position in the neonatal period vs. the upright position in childhood. Even taking into account these technical problems, however, we believe that our quantitative analyses, particularly the measurement of the CHA, are a valid way to characterize the distinctive thoracic deformity in upd(14)pat.

Conclusion

The coat-hanger sign of upd(14)pat was quantitatively represented by CHA, and was found to be more severe than that seen in other genetic bone diseases and to persist into early childhood; thus, the findings will help in the diagnosis of upd(14)pat even after infancy. By contrast, the bell-shaped thorax represented by M/W ratio was significant only in the neonatal period, and its diagnostic value declined with age.

References

1. Kotzot D (2004) Advanced parental age in maternal uniparental disomy (UPD): implication for the mechanism of formation. Eur J Hum Genet 12:343–346
2. Towner D, Yang SP, Shaffer G (2001) Prenatal ultrasound findings in a fetus with paternal uniparental disomy 14q12-qter. Ultrasound Obstet Gynecol 18:268–271
3. Offiah AC, Cornette L, Hall CM (2003) Paternal uniparental disomy 14: introducing the "coat-hanger" sign. Pediatr Radiol 33:509–512
4. Stevenson DA, Brothman AR, Chen Z et al (2004) Paternal uniparental disomy of chromosome 14: confirmation of a clinically-recognizable phenotype. Am J Med Genet A 130A:88–91
5. Kagami M, Nishimura G, Okuyama T et al (2005) Segmental and full paternal isodisomy for chromosome 14 in three patients: narrowing the critical region and implication for the clinical feature. Am J Med Genet A 138A:127–132
6. Kurosawa K, Sasaki H, Yamanaka M et al (2002) Paternal UPD 14 is responsible for a distinctive malformation complex. Am J Med Genet 110:268–272
7. Yamanaka M, Ishikawa H, Saito K et al (2010) Prenatal findings of paternal uniparental disomy 14: report of four patients. Am J Med Genet 152A:789–791
8. Sutton VR, McAlister WH, Bertin TK et al (2003) Skeletal defect in paternal uniparental disomy for chromosome 14 are re-capitulated in the mouse model (paternal uniparental disomy 12). Hum Genet 113:447–451
9. Mattes J, Whitehead B, Liehr T et al (2007) Paternal uniparental isodisomy for chromosome 14 with mosaicism for a supernumerary marker chromosome 14. Am J Med Genet 143A:2165–2171
10. Irving MD, Bulting K, Kanber D et al (2010) Segmental paternal uniparental disomy (patUPD) of 14q32 with abnormal methylation elicites the characteristic features of complete pat UPD14. Am J Med Genet 152A:1942–1950
11. Georgiades P, Watkins M, Surani MA et al (2000) Parental origin-specific developmental defects in mice with uniparental disomy for chromosome 12. Development 127:4719–4728
12. Kagami M, Sekita Y, Nishimura G et al (2008) Deletions and epimutations affecting the human 14q32.2 imprinted region in individuals with paternal and maternal upd(14)-like phenotypes. Nat Genet 40:237–242
13. Spranger JW (2002) Asphyxiating thoracic dysplasia. In: Spranger JW, Brill PW, Poznanski A (eds) Bone dysplasia, an atlas of genetic disorders of skeletal development, 2nd edn. Oxford University Press, New York, pp 125–129
14. Swischuk LW (2004) Chapter 1. Respiratory system; respiratory distress in the newborn. In: Swischuk LE (ed) Imaging of the newborn, infant, and young child, 5th edn. Lippincott, Williams & Wilkins, Philadelphia, pp 29–36
15. Cotter PD, Kaffe S, McCurdy LD et al (1997) Paternal uniparental disomy for chromosome 14: a case report and review. Am J Med Genet 70:74–79

Journal of Human Genetics (2011) 56, 566–571

www.nature.com/jhg

ORIGINAL ARTICLE

Maternal age effect on the development of Prader–Willi syndrome resulting from upd(15)mat through meiosis 1 errors

Keiko Matsubara[1,2,3], Nobuyuki Murakami[2,3], Toshiro Nagai[2] and Tsutomu Ogata[1]

Prader–Willi syndrome (PWS) is primarily caused by deletions involving the paternally derived imprinted region at chromosome 15q11.2–q13 and maternal uniparental disomy 15 (upd(15)mat). The underlying mechanisms for upd(15)mat include trisomy rescue (TR), gamete complementation (GC), monosomy rescue and post-fertilization mitotic error, and TR/GC is mediated by non-disjunction at maternal meiosis 1 (M1) or meiosis 2 (M2). Of these factors involved in the development of upd(15)mat, M1 non-disjunction is a maternal age-dependent phenomenon. We studied 117 Japanese patients with PWS and identified deletions in 84 patients (Deletion group) and TR/GC type upd(15)mat through M1 non-disjunction in 15 patients (TR/GC (M1) group), together with other types of abnormalities. Maternal age was significantly higher in TR/GC (M1) group than in Deletion group (median (range), 37 (35–45) versus 30 (19–42); $P=1.0\times10^{-7}$). Furthermore, delayed childbearing age became obvious since the year 2003 in Japan, and relative frequency of TR/GC (M1) group was significantly larger in patients born since the year 2003 than in those born until the year 2002. The results imply that the advanced maternal age at childbirth is a predisposing factor for the development of upd(15)mat because of increased M1 errors.
Journal of Human Genetics (2011) **56**, 566–571; doi:10.1038/jhg.2011.59; published online 2 June 2011

Keywords: maternal age effect; meiosis 1; non-disjunction; Prader-Willi syndrome; upd(15)mat

INTRODUCTION

Prader–Willi syndrome (PWS) is a developmental disorder associated with various dysmorphic, neurologic, cognitive, endocrine and behavioral/psychiatric features.[1] It is caused by absent expression of paternally derived genes on the imprinted region at chromosome 15q11.2–q13, and previous studies have indicated that deletions of the paternally derived imprinted region and maternal uniparental disomy 15 (upd(15)mat) account for ~70 and ~25% of PWS patients, respectively.[1] The remaining PWS patients have rare abnormalities such as epimutations (hypermethylation) of the PWS imprinting center (IC), at the differentially methylated region encompassing exon 1 of *SNRPN* and microdeletions involving the PWS-IC or HBII-85 small nucleolar RNAs distal to the PWS-IC.[2–4]

Upd(15)mat are primarily caused by four mechanisms; that is, trisomy rescue (TR), gamete complementation (GC), monosomy rescue (MR) and post-fertilization mitotic error (PE).[5] TR refers to a condition in which chromosome 15 of paternal origin is lost from a zygote with trisomy 15, formed by fertilization between a disomic oocyte and a normal sperm. GC results from fertilization of a disomic oocyte with a nullisomic sperm. MR refers to a condition in which chromosome 15 of maternal origin is replicated in a zygote with monosomy 15, formed by fertilization between a normal oocyte and a nullisomic sperm. PE is an event after formation of a normal zygote. In this regard, a disomic oocyte specific to TR and GC is produced by non-disjunction at meiosis 1 (M1) or meiosis 2 (M2), and non-disjunction at M1 is known to increase with maternal age, probably because of a long-term (10–50 years) meiotic arrest at prophase 1.[6]

It is predicted, therefore, that the relative frequency of TR/GC-type upd(15)mat through M1 non-disjunction is high in PWS patients born to aged mothers and is increasing in countries where childbearing age is rising. In this context, previous studies have revealed a significantly higher maternal age in PWS patients with upd(15)mat than in those with deletions,[7,8] a significantly higher relative frequency of upd(15)mat in patients born to mothers aged ⩾35 years than in those born to mothers aged <35 years[9] and a significantly increased relative frequency of upd(15)mat in PWS patients <5 years of age in United Kingdom where childbearing age is increasing.[10] In these

[1]Department of Molecular Endocrinology, National Research Institute for Child Health and Development, Tokyo, Japan and [2]Department of Pediatrics, Dokkyo Medical University Koshigaya Hospital, Saitama, Japan
[3]These authors contributed equally to this work.
Correspondence: Dr T Ogata, Department of Molecular Endocrinology, National Research Institute for Child Health and Development, 2-10-1 Ohkura, Setagaya, Tokyo 157-8535, Japan.
E-mail: tomogata@nch.go.jp
Received 3 March 2011; revised 29 April 2011; accepted 8 May 2011; published online 2 June 2011

studies, however, as underlying mechanisms for upd(15)mat have not been examined, it remains to be clarified whether such maternal age effect on the occurrence of upd(15)mat is primarily mediated by M1 non-disjunction. Furthermore, after studying underlying mechanisms for upd(15)mat by microsatellite analysis, Robinson *et al.*[11] have mentioned that maternal age effect is similar between M1 and M2 errors. Thus, it remains to be clarified whether advanced maternal age is relevant to the occurrence of TR/GC type upd(15)mat through M1 errors.

Here, we report that the advanced maternal age at childbirth constitutes a risk factor for TR/GC type upd(15)mat through M1 non-disjunction.

MATERIALS AND METHODS

This study was approved by the Institute Review Board Committees at the National Center for Child Health and Development and Dokkyo University Koshigaya Hospital, and performed after obtaining informed consent.

PWS patients

This study consisted of 117 Japanese PWS patients (72 male patients and 45 female patients) who satisfied the following selection criteria: (1) normal karyotype in all the 50 lymphocytes examined, (2) hypermethylated PWS-IC that was confirmed by methylation analysis for bisulfite-treated leukocyte genomic DNA, using methylated and unmethylated allele-specific PCR primers (Supplementary Figure 1),[12] and (3) positive data on the maternal age at childbirth (parental age was not found in two aged patients who had left our follow-up and whose hospital records had been discarded and in one patient who was born after artificial insemination by donor).

Molecular studies

We performed fluorescence *in situ* hybridization analysis, microsatellite analysis and multiplex ligation-dependent probe amplification (MLPA) analysis. For fluorescence *in situ* hybridization analysis, an ~125-kb probe identifying a region encompassing *SNRPN* was hybridized to lymphocyte metaphase spreads, together with a CEP 15 probe for *D15Z1* and a probe for *PML* on 15q22 utilized as internal controls. The probe for the *SNRPN* region was labeled with digoxigenin and detected by rhodamine anti-digoxigenin, and the control probes were detected according to the manufacturer's protocol (Abbott, Chicago, IL, USA). For microsatellite genotyping, PCR amplification was performed for 13 microsatellite loci on chromosome 15, using fluorescently labeled forward primers and unlabeled reverse primers. Subsequently, the PCR products were determined for size on a CEQ8000 autosequencer (Beckman Coulter, Fullerton, CA, USA). For MLPA analysis, we utilized a commercially available MLPA probe mix (ME028-B1) for multiple segments on the chromosome 15 imprinted region, including the PWS-IC and three portions within the HBII-85 small nucleolar RNAs (MRC-Holland, Amsterdam, The Netherlands). The procedure was as described in the manufacturer's instructions. The primers utilized in this study are summarized in Supplementary Table 1.

Classification of PWS patients

The PWS patients were classified into several groups, according to the underlying (epi) genetic causes (Figure 1). In particular, upd(15)mat was divided into three groups by the previously reported methods[13] (Supplementary Figure 2): (1) heterodisomy for at least one of the three adjacent pericentromeric (<4 Mb from the centromere) microsatellite loci (*D15S541*, *D15S542* and *D15S1035*) was regarded as indicative of TR/GC type upd(15)mat through M1 non-disjunction (TR/GC (M1) group), (2) the combination of isodisomy for the pericentromeric microsatellite loci and heterodisomy for at least one middle to distal microsatellite loci was interpreted as indicative of TR/GC type upd(15)mat through M2 non-disjunction (TR/GC (M2) group) and (3) isodisomy for all the informative microsatellite loci was regarded as indicative of MR/PE type upd(15)mat (MR/PE group). However, it is usually impossible to distinguish between TR and GC, and between MR and PE on the basis of microsatellite data, although identification of segmental isodisomy or mosaicism with a normal cell lineage is unique to PE.[14,15]

Analysis of parental ages

We compared parental ages between different groups and between two different time periods (until the year 2002 and since the year 2003), and relative frequency of each group between the two time periods. The setting of the two time periods was based on the Annual Vital Statistics Data from the Japanese Ministry of Health, Labor and Welfare (http://www.mhlw.go.jp/toukei/list/81-1.html). The maternal age producing the largest number of live births changed from 25–29 years to 30–34 years, and that producing the third largest number of live births changed from 20–24 years to 35–39 years, between the two time periods (Supplementary Figure 3).

Statistical significance of the median age was examined by the Mann–Whitneys *U*-test, that of the correlation between parental ages by Spearman's rank correlation test, and that of relative frequency by the Fisher's exact probability test. $P<0.05$ was considered significant.

RESULTS

Classification of PWS patients

The results are shown in Figure 1. Fluorescence *in situ* hybridization analysis revealed heterozygous deletions in 84 of the 117 patients (Supplementary Figure 4;Deletion group). Then, microsatellite genotyping was carried out in 27 of the 33 patients without deletions, classifying 15 patients as TR/GC (M1) group, seven patients as TR/GC (M2) group and three patients as MR/PE group (Figure 2;in the remaining six patients, further studies were refused by the parents). There was no finding indicative of segmental isodisomy or mosaicism. Finally, MLPA was performed in the remaining two non-upd(15)mat patients, identifying no microdeletion affecting the PWS-IC. Thus, the two patients were classified as Epimutation group.

Analysis of parental ages

Distribution of parental ages in each group is shown in Figure 3a, and parental age data are summarized in Table 1. Maternal ages were invariably ⩾35 in TR/GC (M1) group. Furthermore, comparison of maternal ages in Deletion, TR/GC (M1) and TR/GC (M2) groups with >5 patients revealed significant difference between Deletion and TR/GC (M1) groups ($P=1.0\times10^{-7}$), but not between Deletion and TR/GC (M2) groups ($P=0.19$), and between TR/GC (M1) and TR/GC (M2) groups ($P=0.085$). Paternal ages showed similar tendency, with

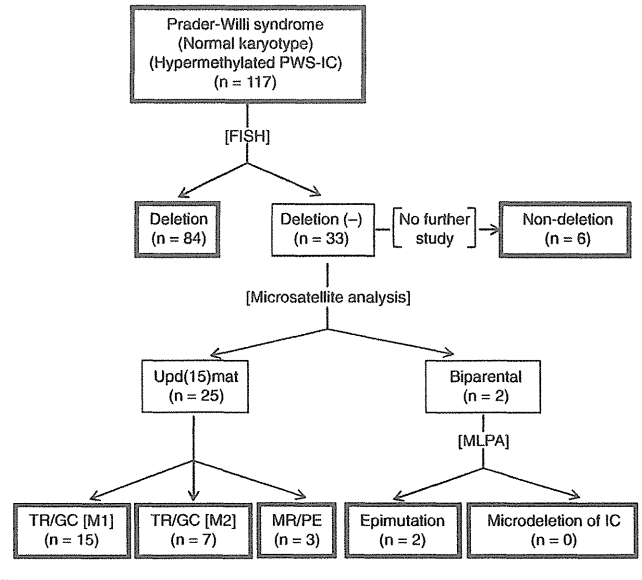

Figure 1 Classification of 117 Japanese patients with Prader–Willi syndrome phenotype.

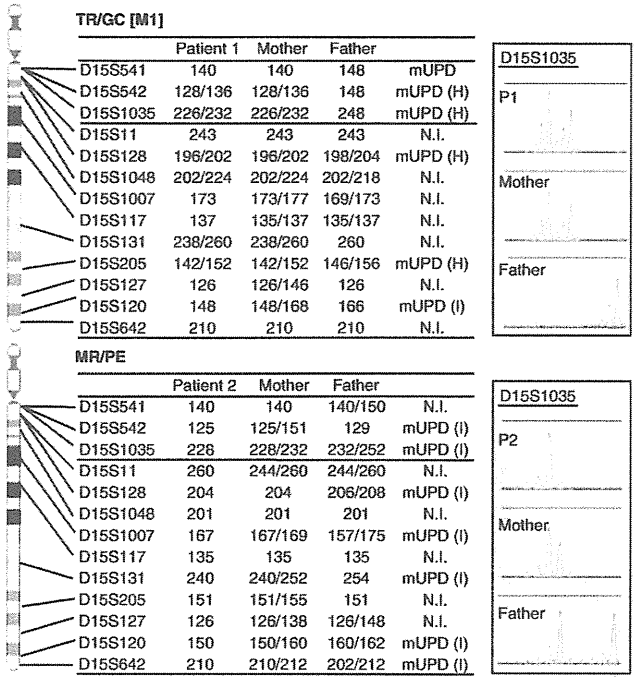

Figure 2 Chromosomal locations of the examined microsatellite loci and representative results. MUPD, maternal uniparental disomy (unknown for heterodisomy or isodisomy); mUPD (H), maternal uniparental heterodisomy; mUPD (I), maternal uniparental isodisomy; N.I., not informative. Pericentromeric loci are present in a heterodisomic status in patient 1, and this is consistent with trisomy rescue/gamete complementation (meiosis 1) (TR/GC (M1)) type maternal uniparental disomy 15 (upd(15)mat). For D15S1035, for example, both of the heterozygous maternal alleles are inherited by patient 1, whereas the homozygous paternal alleles are not transmitted to patient 1; this demonstrates mUPD (H) for this locus. In patient 2, all informative loci are present in an isodisomic condition, and this is compatible with monosomy rescue/post-fertilization mitotic error (MR/PE) type upd(15)mat. For D15S1035, for example, one of the two heterozygous maternal alleles is transmitted to patient 2, whereas both of the heterozygous paternal alleles are not inherited by patient 2; this demonstrates mUPD (I) for this locus.

significant difference between Deletion and TR/GC (M1) groups ($P=8.8\times10^{-5}$), but not between Deletion and TR/GC (M2) groups ($P=0.39$), and between TR/GC (M1) and TR/GC (M2) groups ($P=0.39$). However, whereas a significant correlation was observed between maternal and paternal ages in Deletion and TR/GC (M2) groups, there was no significant correlation between maternal and paternal ages in TR/GC (M1) group because of relatively advanced maternal ages in this group (Figure 3b). In addition, whereas maternal ages at childbirth were grossly similar between Deletion and TR/GC (M2) groups and the Japanese general population (the mean parental ages at childbirth in Japan were based on the data registered in the Ministry of Health, Labor and Welfare; http://www.mhlw.go.jp/toukei/list/81-1.html), they were obviously higher in TR/GC (M1) group than in the Japanese general population. Paternal ages at childbirth were grossly similar between Deletion group and the Japanese general population and tended to be higher in TR/GC (M1) and TR/GC (M2) groups than in the Japanese general population.

Relative frequency of each group markedly differed between 75 patients born until 2002 and 42 patients born since 2003 (Figure 3c). Here, TR/GC (M1) was indicated in three of the 75 patients born until the year 2002, and six non-deletion type patients were invariably born until the year 2002. Thus, TR/GC (M1) group accounted for at least three and up to nine of the 75 patients born until the year 2002, and 12 of the 42 patients born since the year 2003. Thus, the relative frequency of TR/GC (M1) was assessed to be significantly different, with the *P*-values being 1.8×10^{-7} for 3/75 versus 12/42, and 0.025 for 9/75 versus 12/42. In addition, there was no significant change in the parental ages of each group between the two time periods, although the maternal ages at birth of all the patients significantly differed between the two time periods.

DISCUSSION

The present study revealed deletions in 84 patients, upd(15)mat in 25 patients and epimutations in 2 patients. In addition, whereas microsatellite and MLPA analyses were not performed in six patients with non-deletion, the present and the previous studies argue that most of them have upd(15)mat, especially TR/GC (M1) type upd(15)mat.[1,13] Thus, the relative frequency of deletions, upd(15)mat and other rare causes appears to be similar between Japanese patient and previously reported Caucasian patients.[1]

Notably, the present study implies that advanced maternal age at childbirth constitutes a risk factor for the development of TR/GC (M1) type upd(15)mat. Indeed, maternal ages were significantly higher in TR/GC (M1) group than in Deletion group, which is free from maternal age effect. Although a significant difference was not found between maternal age-dependent TR/GC (M1) group and maternal age-independent TR/GC (M2) group, this would primarily be due to the small number of TR/GC (M2) group. Furthermore, the relative frequency of TR/GC (M1) group significantly increased since the year 2003 when delayed childbearing age became obvious, and the advanced maternal ages at birth since the year 2003 were primarily associated with the high frequency of TR/GC (M1) group rather than the advanced maternal ages in each group. Although it was impossible to distinguish between TR and GC, and between MR and PE,[16] this would not pose a major problem. The patients with M1 non-disjunction are included only in TR/GC (M1) group.

Paternal and environmental factors should also be considered for the present results. For a paternal factor, the frequencies of microdeletions and nullisomic sperms might increase with age.[17] However, paternal ages at childbirth in each group were similar between the two time periods, and the relative frequency of Deletion group actually decreased since the year 2003. Furthermore, whereas nullisomic sperms can be a background of the development of GC, concomitant occurrence of a nullisomic sperm and a disomic oocyte must be extremely rare. Rather, nullisomic sperms would primarily constitute an underlying factor for the development of maternal age-independent MR. For an environmental factor, it is predicted that chemical materials are increasing with time and that aged parents are exposed to such materials for a long time. In this regard, it has been reported that exposure to environmental chemicals may exaggerate the occurrence of aneuploidies in females.[18] Thus, the environmental factor might be relevant to the recent increase of TR/GC (M1) group, although it is unlikely that this factor constitutes the major cause of the increased TR/GC (M1) type upd(15)mat. In males, whereas it has been reported that exposure to chemical materials might facilitate the occurrence of PWS, the relative frequency of genetic causes remained unchanged in PWS patients born to such males.[19–21] Collectively, the effects of such non-maternal age factors would remain small, if any, although further careful examinations are required for the precise evaluation of the maternal age effect on the occurrence of TR/GC (M1).

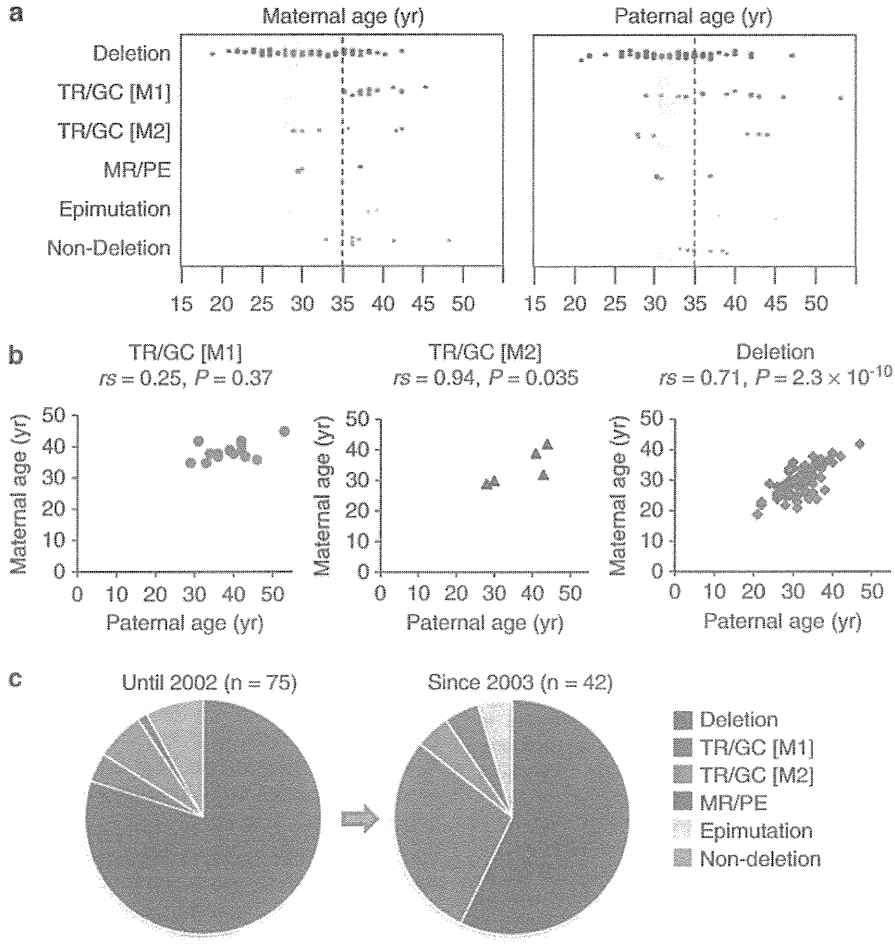

Figure 3 Analysis of parental ages at childbirth. (**a**) The distribution of parental ages in each group. The light pink and blue vertical bars represent the mean maternal and paternal ages at childbirth from the year 1970 to the year 2008. (**b**) Correlation between maternal and paternal ages at childbirth. Significant correlation is observed in trisomy rescue/gamete complementation (meiosis 2) (TR/GC (M2)) and Deletion groups, but not in trisomy rescue/gamete complementation (meiosis 1) (TR/GC (M1)) group because of relatively advanced maternal age. (**c**) Relative frequency of each group in 75 patients born until the year 2002 (n=60, 3, 5, 1, 0 and 6 for Deletion, TR/GC (M1), TR/GC (M2), monosomy rescue/post-fertilization mitotic error (MR/PE), epimutation and non-deletions groups, respectively) and in 42 patients born since the year 2003 (n=24, 12, 2, 2, 2 and 0 for Deletion, TR/GC (M1), TR/GC (M2), MR/PE, Epimutation and Non-deletions groups, respectively).

Several points should be made with regard to the present study. First, we classified upd(15)mat primarily on the basis of the results of three pericentromeric microsatellite loci, with the assumption of no recombination between the centromere and the three loci, as have been employed in the previous study.[13] The methods would be basically acceptable, because the three loci reside within a 4 Mb region from the centromere and a recombination is relatively rare in the centromeric regions.[22] However, it remains possible that a cryptic recombination(s) might have occurred in the pericentromeric region.

Second, upd(15)mat may also be caused by maternal age-dependent meiotic sister chromatid pre-division that can lead to aneuploid oocytes, including disomic oocytes specific to TR/GC.[23] In this regard, as such disomic oocytes can have various patterns of isodisomic and heterodisomic regions, it is impossible to discriminate between upd(15)mat through sister chromatid pre-division and that through conventional meiotic non-disjunction by microsatellite analysis. Thus, the patients classified as TR/GC (M1) group may have upd(15)mat due to maternal age-dependent conventional non-disjunction at M1 and maternal age-dependent sister chromatid pre-division, whereas those classified as TR/GC (M2) group may have upd(15)mat due to maternal age-independent conventional non-disjunction at M2 and maternal age-dependent sister chromatid pre-division. However, even if not all the patients classified as TR/GC (M1) group have upd(15)mat due to conventional non-disjunction at M1, it can be concluded that maternal age-dependent factors still have a critical role in the occurrence of upd(15)mat in patients classified as TR/GC (M1) group. In addition, possible mixture of maternal age-dependent and -independent factors in patients classified as TR/GC (M2) group may be relevant to the lack of significant difference in the maternal age between TR/GC (M2) and Deletion groups, and between TR/GC (M2) and TR/GC (M1) groups.

Lastly, whereas fluorescence *in situ* hybridization analysis has been routinely performed at commercial laboratories since the year 1993 in Japan, detailed molecular studies including microsatellite analysis are usually available only in institutional laboratories. Thus, a substantial fraction of patients without deletions may have remained undiagnosed or misdiagnosed, without receiving further studies including micro-

Table 1 Parental ages (year) at childbirth

	Deletion	*TR/GC (M1)*	*TR/GC (M2)*	*MR/PE*	*Epimutation*	*Non-deletion*	*All patients*	*General population*
Maternal age								
Total								
Median	30	37	31	30	38.5	36	32	27.5–30.9
Range	19–42	35–45	29–42	29–37	38–39	30–48	19–48	
Number	84	15	7	3	2	6	117	
Until 2002								
Median	29	37	32	29	—	36	30[a]	
Range	19–42	35–37	29–42	—	—	30–48	19–48	
Number	60	3	5	1	0	6	75	
Since 2003								
Median	32.5	38.5	35.5	33.5	38.5	—	35[a]	
Range	23–39	35–45	30–41	30–37	38–39	—	23–45	
Number	24	15	2	2	2	0	42	
Paternal age								
Total								
Median	32.5	40	35.5	31	41.5	36	33	30.6–33.0
Range	21–47	29–53	28–44	28–37	38–45	33–39	21–53	
Number	82[b]	15	6[c]	3	2	6	114[b,c]	
Until 2002								
Median	32.5	43	35.5	28	—	36	33	
Range	21–47	33–43	28–44	—	—	33–39	21–47	
Number	58[b]	3	4[c]	1	0	6	72[b,c]	
Since 2003								
Median	32.5	39.5	35.5	34	41.5	—	34.5	
Range	22–40	29–53	30–41	31–37	38–45	—	22–53	
Number	24	12	2	2	2	0	42	

Abbreviations: GC, gamete complementation; M1, meiosis 1; M2, meiosis 2; MR,monosomy rescue; PE, post-fertilization mitotic error; TR, trisomy rescue.
The data of the general population indicate the range of the mean parental ages at childbirth from the year 1970 to 2008.
[a]*P*-value=0.00017.
[b]Paternal age was not found in two old patients who had left our follow-up and whose hospital records had been discarded.
[c]Paternal age was not identified in one patient who was born after artificial insemination by donor.

satellite analysis at appropriate institutions. In this regard, considering the opportunity to receive detailed molecular studies, it is possible that upd(15)mat is overlooked more frequently in aged patients than in young patients. If so, this may be relevant to the significant difference in the relative frequency of TR/GC (M1) group between the two time periods ('since the year 2003' versus 'until the year 2002').

In summary, the results imply that the advanced maternal age at childbirth is a predisposing factor for the development of upd(15)mat because of increased M1 errors. This notion is applicable to maternal upd in general, as well as to trisomies. However, there are several caveats as discussed in the above, and the number of patients, especially those classified as TR/GC (M2) group, is small. Thus, further careful studies using a large number of patients are necessary in the future.

CONFLICT OF INTEREST

The authors declare no conflict of interest.

ACKNOWLEDGEMENTS

This work was supported by Grants for Research on Intractable Diseases (H22-165) and for Health Research on Children, Youth and Families (H21-005) from the Ministry of Health, Labor and Welfare, and by Grants-in-Aid for Scientific Research (A) (22249010) and Grant-in-Aid for Young Scientists (B) (22791022) from the Japan Society for the Promotion of Science (JSPS).

1 Cassidy, S. B. & Driscoll, D. J. Prader-Willi syndrome. *Eur. J. Hum. Genet.* **17,** 3–13 (2009).
2 Buiting, K., Grob, S., Lich, C., Gillessen-Kaesbach, G., El-Maarri, O. & Horsthemke, B. Epimutation in Prader-Willi and Angelman syndromes: a molecular study of 136 patients with an imprinting defect. *Am. J. Hum. Genet.* **72,** 571–577 (2003).
3 Sahoo, T., del Gaudio, D., German, J. R., Shinawi, M., Peter, S. U., Person, R. E. *et al.* Prader-Willi phenotype caused by paternal deficiency for the HBII-85 C/D box small nucleolar RNA cluster. *Nat. Genet.* **40,** 719–721 (2008).
4 de Smith, A. J., Purmann, C., Walters, R. G., Ellis, R. J., Holder, S. E., VanHaelst, M. *et al.* A deletion of the HBII-85 class of small nucleolar RNAs (snoRNAs) is associated with hyperphagia, obesity and hypogonadism. *Hum. Mol. Genet.* **18,** 3257–3265 (2009).
5 Shaffer, L. G., Agan, N., Goldberg, J. D., Ledbetter, D. H., Longshore, J. W. & Cassidy, S. B. American College of Medical Genetics statement on diagnostic testing for uniparental disomy. *Genet. Med.* **3,** 206–211 (2001).
6 Jones, K. T. Meiosis in oocytes: predisposition to aneuploidy and its increased incidence with age. *Hum. Reprod. Update.* **14,** 143–158 (2008).
7 Mitchell, J., Schinzel, A., Langlois, S., Gillessen-Kaesbach, G., Schuffenhauer, S., Michaelis, R. *et al.* Comparison of phenotype in uniparental disomy and deletion Prader-Willi syndrome: sex specific differences. *Am. J. Med. Genet.* **65,** 133–136 (1996).
8 Cassidy, S. B., Forsythe, M., Heeger, S., Nicholls, R. D., Schork, N., Benn, P. *et al.* Comparison of phenotype between patients with Prader-Willi syndrome due to deletion 15q and uniparental disomy 15. *Am. J. Med. Genet.* **68,** 433–440 (1997).
9 Ginsburg, C., Fokstuen, S. & Schinzel, A. The contribution of uniparental disomy to congenital development defects in children born to mothers at advanced childbearing age. *Am. J. Med. Genet.* **95,** 454–460 (2000).
10 Whittington, J. E., Butler, J. V. & Holland, A. J. Changing rates of genetic subtypes of Prader-Willi syndrome in the UK. *Eur. J. Hum. Genet.* **15,** 127–130 (2007).
11 Robinson, W. P., Langlois, S., Schuffenhauer, S., Horsthemke, B., Michaelis, R. C., Christian, S. *et al.* Cytogenetic and age-dependent risk factors associated with uniparental disomy 15. *Prenat. Diagn.* **16,** 837–844 (1996).

12 Kubota, T., Das, S., Cristian, S. L., Baylin, S. B., Herman, J. G. & Ledbetter, D. H. Methylation-specific PCR simplifies imprinting analysis. *Nat. Genet.* **16,** 16–17 (1997).
13 Robinson, W. P., Kuchinka, B. D., Bernasconi, F., Peterson, M. B., Schulze, A., Brondum-Nielsen, K. *et al.* Maternal meiosis I non-disjunction of chromosome 15: dependence of the maternal age effect on level of recombination. *Hum. Mol. Genet.* **7,** 1011–1019 (1998).
14 Robinson, W. P. Mechanisms leading to uniparental disomy and their clinical consequences. *Bioessays* **22,** 452–459 (2000).
15 Kotzot, D. Advanced parental age in maternal uniparental disomy (UPD): implications for the mechanism of formation. *Eur. J. Hum. Genet.* **12,** 343–346 (2004).
16 Oliver, T. R., Feingold, E., Yu, K., Cheung, V., Tinker, S., Yadav-Shah, M. *et al.* New insights into human nondisjunction of chromosome 21 in oocytes. *PLoS Genet.* **4,** e1000033 (2008).
17 Sloter, E., Nath, J., Eskenazi, B. & Wyrobek, A. J. Effects of male age on the frequencies of germinal and heritable chromosomal abnormalities in humans and rodents. *Fertil. Steril.* **81,** 925–943 (2004).
18 Pacchierotti, F., Adler, I. D., Eichenlaub-Ritter, U. & Mailhes, J. B. Gender effects on the incidence of aneuploidy in mammalian germ cells. *Environ. Res.* **104,** 46–69 (2007).
19 Strakowski, S. M. & Butler, M. G. Paternal hydrocarbon exposure in Prader-Willi syndrome. *Lancet* **330,** 1458 (1987).
20 Cassidy, S. B., Gainey, A. J. & Butler, M. G. Occupational hydrocarbon exposure among fathers of Prader-Willi syndrome patients with and without deletions of 15q. *Am. J. Hum. Genet.* **44,** 806–810 (1989).
21 Akefeldt, A., Anvret, M., Grandell, U., Nordlinder, R. & Gillberg, C. Parental exposure to hydrocarbons in Prader-Willi syndrome. *Dev. Med. Chil. Neurol.* **37,** 1101–1109 (1995).
22 Robinson, W. P., Bernasconi, F., Mutirangura, A., Ledbetter, D. H., Langlois, S., Malcom, S. *et al.* Nondisjunction of chromosome 15: origin and recombination. *Am. J. Hum. Genet.* **53,** 740–751 (1993).
23 Pellestor, F., Andreo, B., Anahory, T. & Hamamah, S. The occurrence of aneuploidy in human: lessons from the cytogenetic studies of human oocytes. *Eur. J. Med. Genet.* **49,** 103–116 (2006).

Supplementary Information accompanies the paper on Journal of Human Genetics website (http://www.nature.com/jhg)

Proximal Promoter of the Cytochrome P450 Oxidoreductase Gene: Identification of Microdeletions Involving the Untranslated Exon 1 and Critical Function of the SP1 Binding Sites

Shun Soneda,* Takashi Yazawa,* Maki Fukami,* Masanori Adachi, Michiyo Mizota, Kenji Fujieda, Kaoru Miyamoto, and Tsutomu Ogata

Department of Molecular Endocrinology (S.S., M.F., T.O.), National Research Institute for Child Health and Development, Tokyo 157-8535, Japan; Department of Pediatrics (S.S.), St. Marianna University School of Medicine, Kawasaki 216-8511, Japan; Department of Biochemistry, Faculty of Medical Sciences (T.Y., K.M.), University of Fukui, Fukui 910-1193, Japan; Division of Endocrinology and Metabolism (M.A.), Kanagawa Children's Medical Center, Yokohama 232-8555, Japan; Department of Pediatrics (M.M.), Kagoshima University School of Medicine, Kagoshima 890-8520, Japan; Department of Pediatrics (K.F.), Asahikawa Medical Collage, Asahikawa 078-8510, Japan; and Department of Pediatrics (T.O.), Hamamatsu University School of Medicine, Hamamatsu 431-3192, Japan

Context: *POR* (cytochrome P450 oxidoreductase) is a ubiquitously expressed gene encoding an electron donor to all microsomal P450 enzymes and several non-P450 enzymes. *POR* mutations cause an autosomal recessive disorder characterized by skeletal dysplasia, adrenal dysfunction, and disorders of sex development. Although recent studies have indicated the presence of a CpG-rich region characteristic of housekeeping genes around the untranslated exon 1 (exon 1U) and a tropic effect of thyroid hormone on *POR* expression via thyroid hormone receptor-β, detailed regulatory mechanisms for the *POR* expression remain to be clarified.

Objective: Our objective was to report a pivotal element of the proximal promoter of *POR*.

Results: We first studied three patients (cases 1–3) with POR deficiency due to compound heterozygosity with an p.R457H mutation and transcription failure of an apparently normal allele, by oligoarray comparative genomic hybridization and serial direct sequencing of the deletion fusion points. Consequently, a 2,487-bp microdeletion involving exon 1U was identified in case 1 and an identical 49,604-bp deletion involving exon 1U and exon 1 was found in cases 2 and 3. We next analyzed the 2,487-bp region commonly deleted in cases 1–3 by *in silico* analysis, DNA binding analysis, luciferase assays, and methylation analysis. The results showed a critical function of the evolutionally conserved SP1 binding sites just upstream of exon 1U, especially the binding site at the position −26/−17, in the transcription of *POR*.

Conclusions: The results suggest that the SP1 binding sites constitute an essential element of the *POR* proximal promoter. (*J Clin Endocrinol Metab* 96: E1881–E1887, 2011)

Cytochrome P450 (CYP) oxidoreductase (POR) deficiency (PORD) is a rare autosomal recessive disorder caused by mutations in the gene encoding a flavoprotein that functions as an electron donor to all microsomal P450 enzymes and several non-P450 enzymes (1–3). Salient clinical features of PORD include skeletal dysplasia referred to as Antley-Bixler syndrome, adrenal dysfunction, 46,XY and 46,XX disorders of sex development (DSD), and maternal virilization during pregnancy (1–4). Such features are primarily explained by impaired activities of POR-

ISSN Print 0021-972X ISSN Online 1945-7197
Printed in U.S.A.

doi: 10.1210/jc.2011-1337 Received April 25, 2011. Accepted August 18, 2011.
First Published Online September 7, 2011

* S.S., T.Y., and M.F. contributed equally to this work.

Abbreviations: CGH, Comparative genomic hybridization; CYP, cytochrome P450; DSD, disorders of sex development; exon 1U, untranslated exon 1; HEK, human embryonic kidney; POR, CYP oxidoreductase; PORD, POR deficiency; SL2, Schneider line 2.

dependent CYP51A1 and squalene epoxidase involved in cholesterologenesis and CYP17A1, CYP21A2, and CYP19A1 involved in steroidogenesis (1–4). Anorectal and urinary anomalies are also occasionally observed in PORD, probably due to decreased activity of CYP26 relevant to retinoic acid metabolism (5). The complete absence of POR activity is assumed to be lethal (4), and consistent with this, all the patients identified to date have at least one missense mutation that is likely to preserve some residual activity (1, 2, 6, 7). In addition, heterozygosity with one apparently normal allele has been reported in approximately 12% of PORD patients (4).

The *POR/Por* gene is transcribed ubiquitously with more or less variable expression levels among different tissues (8, 9). Consistent with the ubiquitous expression pattern, rat *Por* is known to be associated with a CpG-rich region (CpG islands) (9) characteristic of housekeeping genes (10). Similarly, human *POR* consists of a single untranslated exon 1 (exon 1U) and coding exons 1–15, and the region around exon 1U harbors a CpG-rich region (11). In addition, the SP1 binding sites as a potential proximal promoter element reside in the CpG-rich region of rat *Por* (9), whereas they have not yet been reported in the CpG-rich region of human *POR*. Furthermore, Tee *et al.* (12) have recently studied the approximately 300-bp proximal promoter region just upstream of exon 1U of human *POR*, showing that thyroid hormone exerts a major trophic effect on *POR* expression primarily via thyroid hormone receptor-β, with thyroid hormone receptor-α, estrogen receptor-α, Smad3, and Smad4 exerting lesser modulatory effects. However, the detailed regulatory mechanisms for the transcription of human *POR* remain to be clarified.

Here, we report two types of microdeletions, one involving exon 1U alone and the other involving exon 1U and exon 1, in patients with PORD and suggest a pivotal role of the SP1 binding sites in the transcriptional regulation of *POR*. The results, in conjunction with the previous data (12), provide significant progress in the clarification of the regulatory machinery for the expression of *POR*.

Patients and Methods

Patients

We examined three nonconsanguineous patients (case 1 with 46,XY and cases 2 and 3 with 46,XX) reported in our previous paper describing 35 patients with PORD (7); cases 1, 2, and 3 in this report correspond to cases 18, 26, and 27 in the previous paper, respectively. Cases 1–3 manifested Antley-Bixler syndrome-compatible skeletal features, adrenal dysfunction with

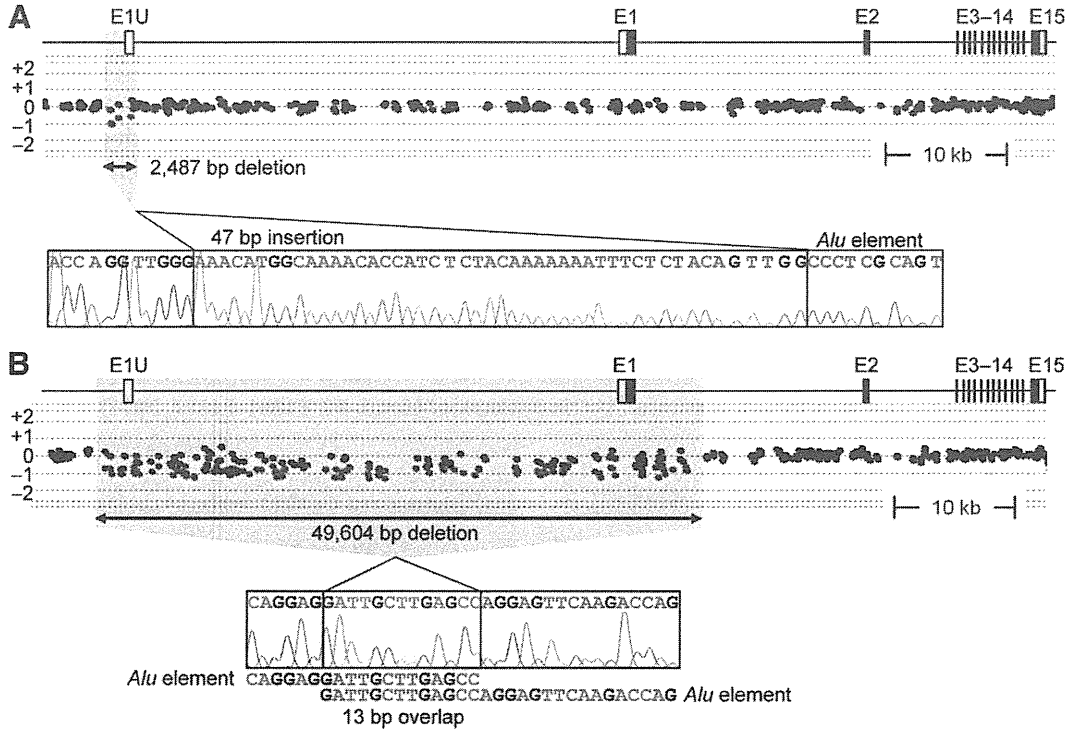

FIG. 1. Identification and characterization of the microdeletions in case 1 (panel A) and cases 2 and 3 (panel B) by CGH analysis and direct sequencing of the deletion junctions. The position of *POR* exons (E1U–E15) is shown on the CGH findings; the *black and white boxes* denote the coding regions and the untranslated regions, respectively. In the CGH results, the *black and green dots* denote signals indicative of the normal and the decreased (<−0.5) copy numbers, respectively. In the direct sequencing findings, the 47-bp segment inserted into the fusion point in case 1 is *highlighted* with *light yellow*, and the 13-bp overlapping sequence at the fusion point in cases 2 and 3 is *highlighted* with *light blue*. The *Alu* elements are indicated with *light blue bars*.